PROCEEDINGS OF SPIE

SPIEDigitalLibrary.org/conference-proceedings-of-spie

Terahertz-to-infrared converter based on the polyvinylchloride matrix with embedded gold nanoparticles

Moldosanov, K., Bykov, A., Kairyev, N., Khodzitsky, M., Kropotov, G., et al.

K. A. Moldosanov, A. V. Bykov, N. Z. Kairyev, M. K. Khodzitsky, G. I. Kropotov, V. M. Lelevkin, I. V. Meglinski, A. V. Postnikov, A. A. Shakhmin, O. Sieryi, "Terahertz-to-infrared converter based on the polyvinylchloride matrix with embedded gold nanoparticles," Proc. SPIE 11868, Emerging Imaging and Sensing Technologies for Security and Defence VI, 118680S (12 September 2021); doi: 10.1117/12.2602089

SPIE.

Event: SPIE Security + Defence, 2021, Online Only

Terahertz-to-infrared converter based on the polyvinylchloride matrix with embedded gold nanoparticles

K.A. Moldosanov[a], A.V. Bykov[b], N.Z. Kairyev[a], M.K. Khodzitsky[c], G.I. Kropotov[c], V.M. Lelevkin[a], I.V. Meglinski[b], A.V. Postnikov[d], A.A. Shakhmin[c], and O. Sieryi[b]

[a]Kyrgyz-Russian Slavic University, Bishkek, Kyrgyzstan
[b]University of Oulu, Oulu, Finland
[c]Tydex LLC, Saint Petersburg, Russia
[d]Université de Lorraine, LCP-A2MC, Metz, France

ABSTRACT

Prospects for the development of devices for visualizing terahertz (THz) radiation sources can be associated with the use of the results of old studies (1965–1978) on the absorption of THz radiation by metal nanoparticles. This "renaissance" demonstrates that metallic nanoparticles can be used as nanotransducers of invisible THz radiation to infrared (IR) radiation detectable by a commercial IR camera. The investigated THz-to-IR converters are matrices that are transparent both in the THz radiation range to be visualized and in the operating range of the IR camera; matrices contain embedded metal nanoparticles. The latter, when irradiated with THz rays, convert the energy of THz photons into heat and become nanosources of IR radiation for the IR camera. In metal nanoparticles, the mechanisms of absorption of THz radiation and its conversion into heat are realized through dissipation of the energy of THz photons due to multiple scattering of electrons, as well as because of excitation of two types of phonons (transverse and longitudinal ones). The conversion of THz energy into the energy of transverse phonons occurs directly, while dissipation and excitation of longitudinal phonons occurs indirectly, through the excitation of Fermi electrons. Polyvinylchloride (PVC) was chosen as the matrix material, and gold nanoparticles were chosen as nanoparticles-fillers.

Keywords: infrared camera, IR, matrix, nanoparticle, phonon, polyvinylchloride, terahertz-to-infrared converter, THz

1. INTRODUCTION

On the scale of electromagnetic (EM) waves, there is a frequency band that is attractive for its potential applications in important areas such as cancer cell imaging and hidden object detection. This is the so-called terahertz (THz) range, placed between radio waves and infrared (IR) radiation. THz radiation has properties inherent to its neighboring bands: it penetrates many optically opaque media, like radio waves, and can be refracted and focused by lenses, like IR rays. Until recently, there were no convenient sources of THz radiation and detectors: radiation generation and detection methods developed for adjacent bands, radio waves and IR, are ineffective in the THz band and face serious problems.

Since some years, we develop the concept and theoretically evaluate the parameters of so-called terahertz-to-infrared (THz-to-IR) converters.[1–8] Once proven operational, such devices would allow a conversion of invisible THz radiation into IR radiation that could be observed with commercial IR cameras. Such systems can be used e.g. for scanning skin cancer (see Fig. 9.2 of Ref. 5 and the related discussion) or for detecting hidden objects on the human body under clothing (see Fig. 6 of Ref. 8) at checkpoints on transport and other public places.

The THz-to-IR converters in question consist of matrices, transparent both in the range of THz radiation to be visualized and in the operating range of the IR camera, the matrices being "stuffed" with metal nanoparticles (see Fig. 1). These latter, when irradiated with THz rays, convert the energy of THz photons into heat and become sources of IR radiation, which can be further on detected by an IR camera.

Further author information: (Send correspondence to K.A.M.)
K.A.M.: E-mail: altair1964@yandex.ru
A.V.P.: E-mail: andrei.postnikov@univ-lorraine.fr

Emerging Imaging and Sensing Technologies for Security and Defence VI, edited by Gerald S. Buller, Richard C. Hollins, Robert A. Lamb, Martin Laurenzis, Proc. of SPIE Vol. 11868, 118680S
 · doi: 10.1117/12.2602089

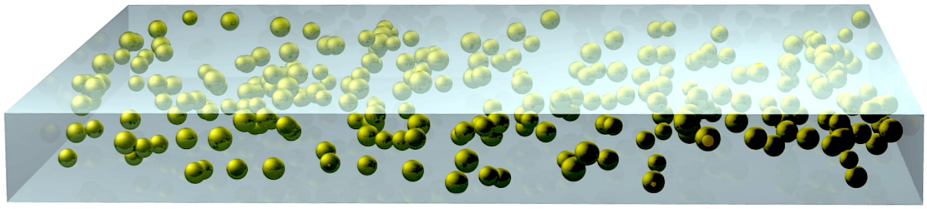

Figure 1. The "working element" of a THz-to-IR converter: a matrix with embedded metal nanoparticles.

In initial works, we suggested to use nanoparticles of nickel[1,2] and Cu-Ni alloys,[3] which have high density of electronic states near the Fermi level, hinting for sufficiently high absorption capacity. However, today it became clear that it would be more convenient to use commercially available gold nanoparticles, which are produced with a fairly small spread of sizes around the nominal one.

We have considered different combinations of materials to be used in THz-to-IR converters. Table 1 specifies the parameters of some of them, chosen so, in order to be specific, as to make use of the temperature sensitivity of $\approx$ 12 mK, inherent for the *Mirage 640 P-series* IR camera, one of broadly used ones.[9] The numerical estimates demonstrate that the converters so suggested might operate on a real-time mode, since the heating and cooling times of the selected nanoparticles are sufficiently small.

Table 1. Comparison of estimated characteristics of the THz-to-IR converters. All data are given for the most practically significant value of the emissivity factor equal to 0.5. The thickness of the Teflon® film was 0.1 mm.

Ref. to article or patent	Parameter					
	Nanoparticle material	Nanoparticle diameter (nm)	Matrix material	Nanoparticle heating / cooling times (ns)	Power required to heat the nanoparticle to be seen by the IR camera (nW)	Frequency of operating radiation (THz)
[1,2]	Ni	2.4	Gelatin	13 / 13	0.13	5 – 7
[3]	Cu – Ni alloy (constantan)	2.5	Gelatin	72 / 78	0.13	0.1 – 10
[4]	Au	2.4	Teflon®	79 / 71	0.11	4.2
[5–7]	Au	8.5	Teflon®	300 / 1281	0.34	0.38; 4.2; 8.7
			Silicon	0.17 / 1.16	98.4	0.38; 4.2; 8.7
[8]	Au	6.0	Teflon®	230 / 1190	0.28	0.7
		9.5		330 / 1360	0.44	0.41
		14.65		430 / 1390	0.68	0.24
		25.4		560 / 1580	1.2	0.14

2. HEATING OF METAL NANOPARTICLES BY THz RADIATION

Unfortunately, there is little data on the absorption of EM THz radiation by metal nanoparticles. Therefore, we turned to old works (1965 – 1978) on absorption by aluminum nanoparticles in the THz frequency range.[10–15]

These experimental and theoretical studies demonstrate the promise of using metal nanoparticles as nanotransducers of THz radiation into IR radiation (heat). We have identified the following physical mechanisms of THz radiation absorption, which may result in nanoparticles' heating:

(i) direct transfer of the energy of EM THz radiation into mechanical energy of vibrations, e.g., into that of transverse phonons: transverse EM waves penetrating into a nanoparticle swing the lattice of ions if at resonance with the frequencies of transverse phonons;

(ii) indirect transformation of the energy of EM THz radiation into mechanical energy of vibrations, e.g., into longitudinal phonons – via excitation of the Fermi electrons;

(iii) simultaneous absorption of a THz photon and a primary longitudinal phonon by a Fermi electron, with a subsequent relaxation of an excited electron by generating a secondary longitudinal phonon whose energy equals the sum of the energies of a THz photon and a primary longitudinal phonon;

(iv) dissipation of the energy acquired by a Fermi electron from a THz photon due to multiple scattering of an excited electron by other electrons.

Although we ultimately turn to gold nanoparticles, rather than the aluminum ones, to be used in THz-to-IR converter, for the sake of better understanding the physical mechanism of nanoparticles heating (i) we will first briefly review Refs. 10–15. The physical mechanism (ii) was considered in Ref. 16, and a variety of realisations of the mechanism (iii) – in Ref. 17. Physical mechanism (iv) takes efect if the energy level of an excited electron does not coincide with any of the energy levels of longitudinal phonons.

Experimental studies of the absorption of EM radiation by aluminum nanoparticles in the frequency ranges of $0 - 1.5$ THz[10] and $0 - 7.5$ THz[11] have shown that the absorption coefficients of aluminum particles with sizes $\sim 10 - 40$ nm in the frequency range ~ 90 GHz $- 4.5$ THz are proportional to the square of the frequency. These results were compared with the prediction of the Gor'kov–Eliashberg theory[12] for particles that took into account the quantization of the energy levels of electrons, as well as with the classical Drude theory. The Gor'kov–Eliashberg theory also predicts a quadratic dependence of the absorption coefficient on the frequency. In fact, the experimental results[10,11] demonstrated that the measured values of the absorption coefficient significantly exceed the predictions of the Gor'kov–Eliashberg theory.

Glick and Yorke have shown in their theoretical work[13] that strong absorption of small metal particles in the THz wavelength range was associated with the direct excitation of phonons due to the action of the EM wave field on the surface ions of the particle. It was noted that the authors of experimental works[10,11] were not able to explain the reason for such a large absorption, which by more than three orders of magnitude exceeded the predictions of both the Gor'kov–Eliashberg and the classical Drude theories. Glick and Yorke[13] for the first time pointed out an issue the authors of Ref. 10, 11 did not pay attention to, and which might account for an unexpectedly strong absorption. They calculated the density of phonon states as a function of their frequency, compared their results with those of Ref. 14, and found a good match. Namely, the results of both studies had a quadratic dependence in the frequency range up to ~ 4 THz (this is the frequency range of transverse phonons). This correlation of the phonon state density profile and the absorption coefficient allowed Glick and Yorke to suggest that a strong absorption in aluminum nanoparticles might be explained by direct excitation of transverse phonons by incident radiation. An explanation lacked, however, as to why the absorption coefficient increased with the particle size. A clue has been given by Granqvist[15] who anticipated, from theory considerations, an increase in the absorption coefficient for aluminum particles with their diameter, in the latter's range of $5 - 100$ nm.

An immediate practical importance of experimental results[10,11,15] for the concept of THz-to-IR convertor is that nanoparticles of various sizes absorb in a broad range (see, e.g. Fig. 3,4 of Ref. 10), therefore an accurate selection of nanoparticle is not a critical issue (they all absorb anyway), and just setting some target spread of particle sizes would be acceptable. With this, the absorption is proportional to the size of the nanoparticles.

Aluminum nanoparticles cannot be used in the THz-to-IR converter because of their pyrophoricity. Therefore, we chose gold nanoparticles for the converter and used the data for aluminum by analogy. In relation to electronic

properties at the Fermi level, with some simplification, gold can be considered as a simple metal. Both metals have the same crystal structure and almost identical lattice parameters. What's more important, gold nanoparticles are commercially available.

Prerequisites for the absorption of EM radiation with the frequency ν by a metal nanoparticle of size D due to the excitation of phonon with the frequency ν are the following:

- the nanoparticle size D is smaller than the penetration depth d of EM radiation with the frequency ν: $D \leq d$;
- the phonon wavelength λ at the frequency of the incident EM radiation ν is not larger than the size D of the nanoparticle: $\lambda \leq D \leq d$;
- the Heisenberg relation for the momenta of a phonon and an electron in a nanoparticle of size D ensures the fulfillment of the law of conservation of momentum upon excitation of a phonon.

D should not be smaller than the size at which spontaneous emission of THz radiation by a (small enough) gold nanoparticle begins, i.e., $D > 8$ nm,[17] in order to prevent the nanoparticle's cooling via emission of THz photons (see also Appendix).

From the results of Ref. 10–15 for aluminum nanoparticles it follows that, if they satisfy the aforementioned prerequisites, an absorption of EM radiation takes place at all wavelengths at which phonons, whether transverse or longitudinal, exist in a nanoparticle. According to the phonon dispersions along the $\Gamma - X$ direction in the reciprocal lattice of gold,[18] the maximum frequencies of longitudinal and transverse phonons are $\approx$ 4.5 THz and $\approx$ 2.55 THz, respectively. Hence, at a frequency of 4.5 THz, the depth of the skin layer is $d = 35.2$ nm, and at a frequency of 2.55 THz, $d = 46.7$ nm. This means that for gold, it is necessary to choose nanoparticles smaller than 35.2 nm, or, more precisely, in the range of $\approx 8 - 35$ nm.

Let us estimate the minimum frequencies of transverse and longitudinal phonons capable of being excited in a gold nanoparticle with a diameter D. We assume that the phonon dispersion curves in gold nanoparticles do not differ from those in bulk gold. Then the propagation velocities of transverse and longitudinal phonons can be estimated from the available dispersion curves of phonons in bulk gold.[18] The wavelengths of transverse and longitudinal phonons are equal, respectively, $\lambda_{\mathrm{T}} = (v_{\mathrm{T}}/\nu)$ and $\lambda_{\mathrm{L}} = (v_{\mathrm{L}}/\nu)$, where v_{T} and v_{L} are, respectively, the propagation velocities of transverse and longitudinal phonons. Since the maximum wavelength that can be excited in a nanoparticle is equal to the diameter D, the minimum frequencies of transverse and longitudinal phonons that can be excited in a nanoparticle are $\nu_{\mathrm{T}}^{(\mathrm{min})} = (v_{\mathrm{T}}/D)$ and $\nu_{\mathrm{L}}^{(\mathrm{min})} = (v_{\mathrm{L}}/D)$, respectively. This directly transposes into the minimum frequency of EM THz radiation absorbable due to the direct excitation of transverse or longitudinal phonons. So, for example, for the 8.5 nm diameter gold nanosphere, assuming for simplicity the $\Gamma - X$ propagation direction (although phonon dispersions in gold are fairly isotropic), we arrive at $\nu_{\mathrm{L}}^{(\mathrm{min})} = 0.38$ THz and $\nu_{\mathrm{T}}^{(\mathrm{min})} = 0.15$ THz, respectively, using the respective $\Gamma - X$ velocities of sound of $v_{\mathrm{L}} = 3.23 \cdot 10^5$ cm/s and $v_{\mathrm{T}} = 1.28 \cdot 10^5$ cm/s.

The size of nanoparticles in the THz-to-IR converter is much smaller than the wavelength of the incident THz radiation. However, the Rayleigh scattering does not occur, since the aforementioned prerequisites for the absorption of EM radiation, $\lambda \leq D \leq d$, are satisfied. Under these conditions, THz radiation will not be scattered into the solid angle of 4π steradian, but will penetrate into the nanoparticle, in which the physical mechanisms of heating $(i) - (iv)$ identified above will set to work.

3. PROPERTIES OF POLYVINYLCHLORIDE MATRIX

Polyvinylchloride (PVC) was chosen as the material of matrix in the present study. Some relevant numerical characteristics of PVC can be found e.g. in the tables of Ref. 19. The transmittance of a 100 μm thick PVC film has been newly measured and depicted (in the frequency range of our present interest) in Fig. 2.

It can be seen that in the wavelength range of 1000 μm and beyond, the transmittance of PVC is interestingly high ($> 80\%$). Therefore, a PVC matrix could be employed in the wavelength range conventionally used to detect

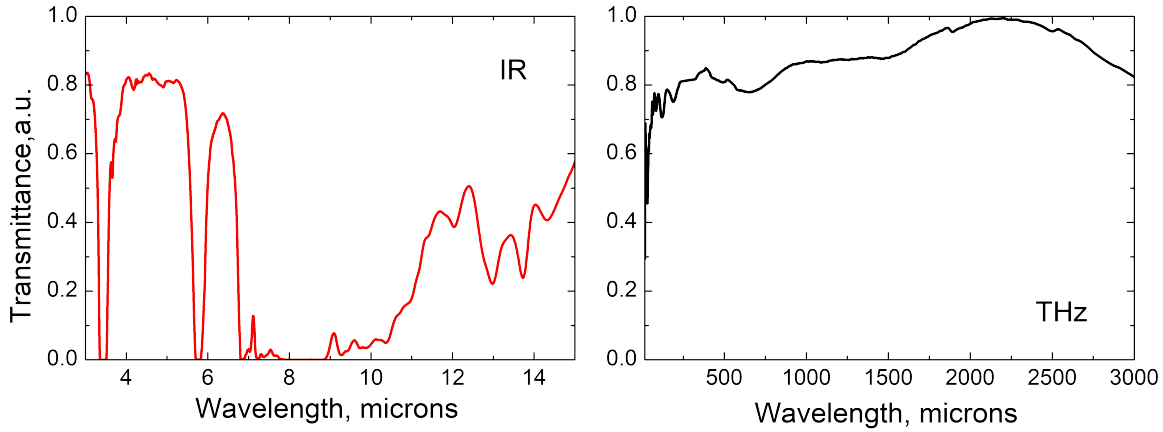

Figure 2. Transmittance of the 100 μm thickness PVC film versus wavelength of IR and THz radiation.

objects hidden under clothing on the human body. We note in passing that the PVC matrix would equally be acceptable for tasks of THz imaging the cancer tissue. Wallace *et al.*[20] and Pickwell and Wallace[21] showed that when biological tissue is irradiated with THz radiation, the maximum contrast in the *refractive index* between the diseased and healthy tissue occurs in the frequency range of $0.35 - 0.55$ THz (corresponding wavelengths: $857 - 545$ μm). Within the same band, there is the maximum difference in the *absorption* of diseased and healthy tissue, which provides the best image contrast.

The transmittance of PVC within the operating wavelengths of commercial IR cameras (e.g., $1.5 - 5$ μm for the *Mirage 640 P-series*[9]) is also quite high but for a narrow dip around $\simeq 3.4$ μm (cf. left panel of Fig. 2). In total, the PVC matrix seems to be a good choice for the THz-to-IR converters.

4. CALCULATIONS OF THE THz-TO-IR CONVERTER PARAMETERS WITH A PVC MATRIX

The calculations were carried out according to the method previously used in Ref. 5. To be specific, we fixed the diameter of embedded gold nanoparticles to 8.5 nm, the same as was already used in Ref. 5 in calculations with two materials for the matrix, silicon and Teflon®, in comparison. We remind that 8.5 nm is beyond the "critical diameter" of a nanoparticle at which (for smaller diameters) the spontaneous emission of THz radiation would occur (see Ref. 17 and the Appendix), offering a channel for the nanoparticles' cooling which is undesirable for the THz-to-IR converter applications.

Table 2 shows the values of the parameters used in the calculations, and Table 3 – the data extracted from the calculations. The emissivity factor α is a phenomenological parameter, difficult to estimate *a priori*, introduced to accont for possible reduction of outcoming emission due to the imperfections of the nanoparticles' shape etc., relative to the theory expectations. The case $\alpha = 1$ corresponds to a nanoparticle being a perfect black body; since in practice it is not a perfect absorber, it is customary to use the value $\alpha = 0.5$ for practical estimations. Fig. 3 depicts graphs of heating and cooling of a gold nanoparticle with a diameter of 8.5 nm in a PVC matrix, and Fig. 4 shows a graph of the final temperature distribution around a gold nanoparticle in a PVC matrix.

Table 2. Parameters of materials used in numerical solutions of the heat equation.

Material	Volume density, $\mathrm{g{\cdot}cm^{-3}}$	Specific heat, $\mathrm{J{\cdot}kg^{-1}K^{-1}}$	Thermal conductivity, $\mathrm{W{\cdot}m^{-1}K^{-1}}$
Nanoparticle : $D = 8.5$ nm gold sphere	$\rho_1 = 19.32$	$C_{1p} = 133.7$	$\lambda_{1p} = 73.65$
Matrix: PVC	$\rho_2 = 1.4$	$C_2 = 1100$	$\lambda_2 = 0.16$

Table 3. Data extracted by solving the heat equation

Emissivity factor α	ΔT, mK	Q, nW	Heating time, 10^{-7} s	Cooling time, 10^{-6} s
1	12	0.103	3.06	1.29
0.5	24	0.207	3.06	1.31

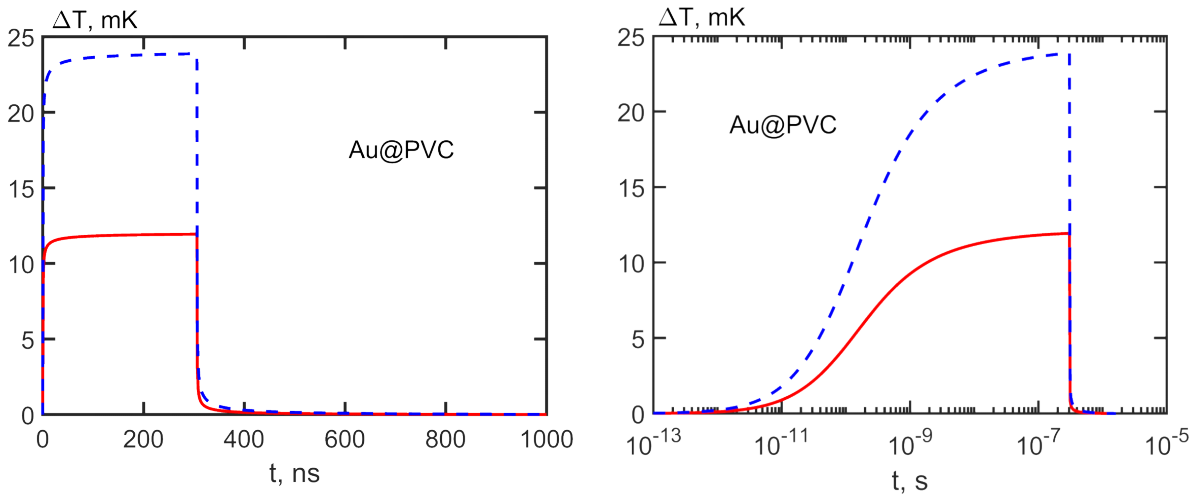

Figure 3. Temperature rise ΔT versus heating/cooling time t for a gold nanoparticle of diameter 8.5 nm in PVC spherical shell for two values of Q from Table 3. Upper curves correspond to emissivity factor of gold nanoparticle $\alpha = 0.5$, lower curves – to $\alpha = 1$. The figure on the right depicts the same functions, using the logarithmic time scale.

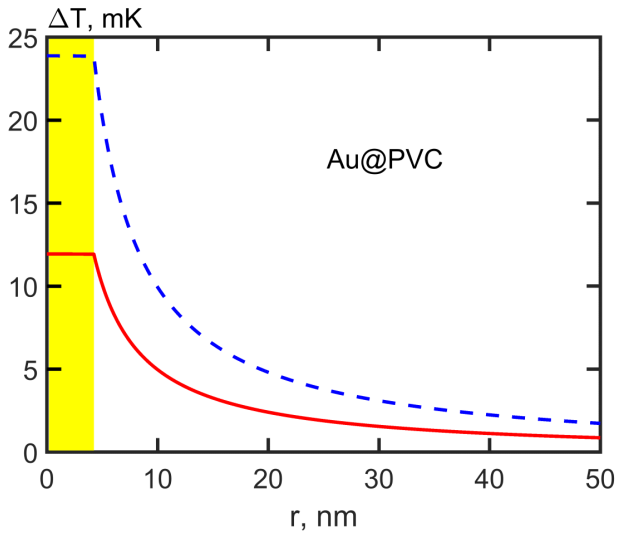

Figure 4. Radial distributions of excess temperatures throughout the gold nanoparticle of diameter 8.5 nm (marked by a colour bar) and its embedding by PVC spherical shell, for the power values of Q from Table 3, corresponding to emissivity factor $\alpha = 1$ (lower curve) and $\alpha = 0.5$ (upper curve).

The heating and cooling times of the 8.5 nm diameter nanoparticle, presented in Table 4 for several matrix materials (to previously discussed Teflon® and silicon, we added gelatin, polystyrene, PVC and polypropylene), are short enough to use a converter in the real-time mode. We note that the values corresponding to embeddings

Table 4. Comparison of estimated parameters of the THz-to-IR converters. In all cases the 8.5 nm diameter gold nanoparticle were used. All data are given for the most practically significant value of the emissivity factor equal to 0.5.

Matrix material	Parameter	
	Nanoparticle heating / cooling times (ns)	Power required to heat the nanoparticle to be seen by the IR camera (nW)
Silicon	0.17/1.16	98.4
Gelatin	407/1718	0.27
Teflon®	300/1281	0.34
Polystyrene	319/1339	0.18
Polypropylene	292/1255	0.25
Polyvinylchloride	306/1314	0.21

in Teflon® (Ref. 5) and in PVC (present calculation) matrices are respectively close. At the same time, the power Q required to heat a nanoparticle so that it would be seen by an IR camera, for a practically significant emissivity factor $\alpha = 0.5$, is about 1.6 times higher for the Teflon® matrix. This will accordingly affect the sensitivity of the THz-to-IR converter on THz power. Therefore, the PVC matrix is more advantageous to use than the Teflon® one.

APPENDIX. SPONTANEOUS EMISSION OF THz PHOTONS BY GOLD NANOPARTICLES

Spontaneous emission of THz photons by gold nanoparticles with diameter less than $\sim$ 8 nm is a manifestation of the size effect and quantization of energy levels of longitudinal phonons under confinement conditions. Consider a compression wave (longitudinal phonon with momentum $\mathbf{q}$) propagating along the nanoparticle diameter D (Fig. 5). Longitudinal phonons with energy E and momentum $\mathbf{q}$ are permanently absorbed by Fermi electrons (assumed to be adequately treated within the free-electron model) with momentum $p_{\rm F} = 1.27{\cdot}10^{-19}$ g·cm/s and energy $E_{\rm F} = 5.53$ eV. The excited (upon absorption) electrons move along the direction characterized by the momentum $\mathbf{s}$, the modulus of which is $s = [2m(E_{\rm F}+E)]^{1/2}$, at an angle γ to the momentum of the phonon (see Fig. 5):

$$\gamma = \arccos\frac{2mE + q^2}{2sq}\,.$$

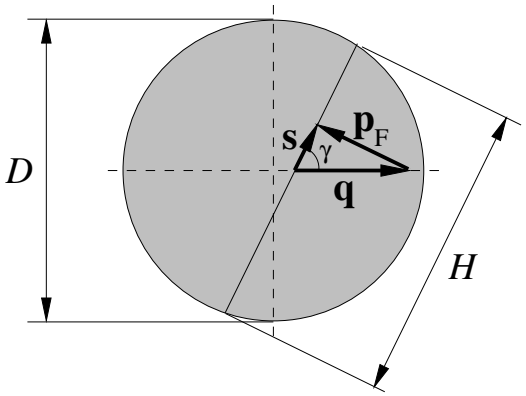

Figure 5. Absorption of the longitudinal phonon with momentum $\mathbf{q}$ by the Fermi electron with momentum $\mathbf{p}_{\rm F}$. The excited electron moves along the direction characterized by the momentum $\mathbf{s}$.

For the longitudinal phonon dominant in gold (with energy $E_0 = 17.4$ meV and magnitude of the momentum $q_0 = 1.13{\cdot}10^{-19}$ g·cm/s), the angle γ is:

$$\gamma = \arccos \frac{2mE_0 + q_0^2}{2sq_0} \approx \frac{q_0}{2p_\mathrm{F}} \approx 0.4449 = 63.6^\circ .$$

Excited electrons, due to the Coulomb interaction with positive ions of gold, could induce secondary longitudinal phonons with momentum collinear to **s**; this would be the relaxation path of excited electrons. However, in nanoparticles smaller than ≈8 nm, this is impossible, and relaxation occurs due to the emission of a photon.

The first reason contributing to emission is the difference in the quantization steps in momenta and energies for longitudinal phonons propagating along the nanoparticle diameter D and along the chord H, collinear to **s**. The momentum steps for phonons propagating along the diameter and along the chord are, respectively, h/D and h/H (h being the Planck's constant). Since $D > H$, the momenta steps are different; consequently, the energy steps for these two directions of phonon propagation do not coincide either. Due to a mismatch of the quantized energy levels, the transfer of energy from the excited electron to the secondary phonon is impossible (the Fermi electron received energy from the primary phonon quantized with a certain step, and it cannot generate a secondary phonon, in which the energy would be quantized with a different step).

Another reason precluding an excitation of secondary phonon and hence favoring the THz emission is the following. As the nanoparticle diameter decreases, the gap between the energy levels of longitudinal phonons for the direction along the vector **s** increases, eventually becoming so large that the gap exceeds the full width at half maximum (FWHM) of the peak of the distribution of longitudinal phonons in energy in gold (Fig. 6 shows the threshold stage of this situation, see details below). As a result, the energy level of an excited electron "hangs" between the levels of longitudinal phonons for the direction **s**: there are none to which it could pass the energy. Consequently, the electron relaxes upon scattering at the nanoparticle boundary, emitting a photon (the electron cannot leave the nanoparticle, since its energy is inferior to the work function of gold, ≈4.8 eV).

For the direction "along the chord H", the steps in momentum and energy of the longitudinal phonons are, respectively, h/H and $\Delta E_H \approx v_\mathrm{L}^*(h/H)$, where v_L^* is the speed of sound for the energy range of longitudinal phonons in the FWHM range. v_L^* is less than the nominal speed of sound in gold, $v_\mathrm{L} = 3.23{\cdot}10^5$ cm/s, due to the bending down of the dispersion curve of longitudinal phonons near the Brillouin zone boundary, where the phonon energies corresponding to FWHM are distributed.

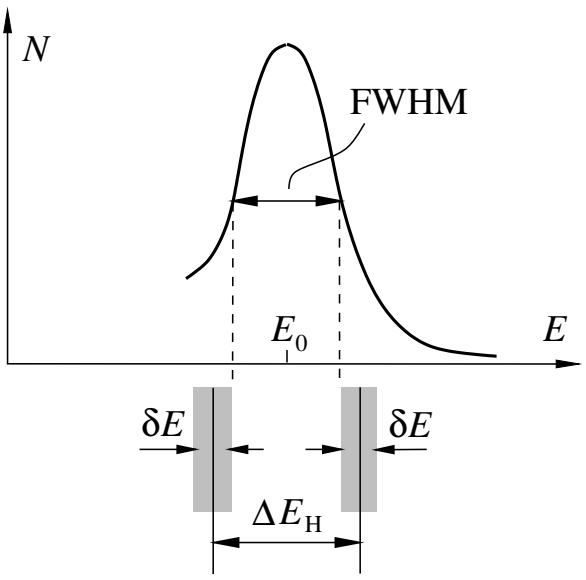

Figure 6. The threshold situation in which the energy step for longitudinal phonons ΔE_H propagating along the vector **s** exceeds the full width at half maximum (FWHM) of the distribution of longitudinal phonons in energy in gold.

Table 5. Relationship between the catalytic activity of a gold nanoparticle and its diameter D.

D (nm)	ΔE_D (meV)	δE (meV)	FWHM/ΔE_D	Note
1.2	3.45	0.55	0.81	Highest catalytic activity
1.5	2.76	0.44	1.01	Decrease in catalytic activity with increasing diameter D
2.5	1.66	0.26	1.69	
5.0	0.83	0.13	3.37	
8.5	0.49	0.08	5.71	Lack of catalytic activity
10.0	0.41	0.07	6.83	

Obviously, the mismatch of energy levels is somehow tempered by the Heisenberg uncertainty relation. We take as a criterion of "total mismatch" between the energy levels of phonons to be potentially excited the situation at which the two consecutive energy levels definitely move apart by more than the FWHM in the (bulk) phonon density of states within the tolerance criteria imposed by the uncertainty relation. Such threshold situation is depicted in Fig. 6, where δE is calculated using the Heisenberg's uncertainty relation for the phonon's momentum and the coordinate, $\delta E \geq v_{\rm L}^* h/(2\pi H)$. The inequality that determines the corresponding threshold chord length (so that at smaller values the spontaneous emission of photons begins to occur) reads as follows:

$$\Delta E_H > \mathrm{FWHM} + (\delta E/2) + (\delta E/2) = \mathrm{FWHM} + \delta E \geq \mathrm{FWHM} + v_{\rm L}^* \frac{h}{2\pi H}\,. \tag{1}$$

Substituting the value $\Delta E_H \approx v_{\rm L}^*(h/H)$ into the left side of inequality (1), we arrive at:

$$v_{\rm L}^*(h/H) > \mathrm{FWHM} + v_{\rm L}^* \frac{h}{2\pi H}\,, \quad \text{or} \qquad H < \left(1 - \frac{1}{2\pi}\right) \frac{v_{\rm L}^* h}{\mathrm{FWHM}}\,. \tag{2}$$

Should this inequality be satisfied, a significant fraction of excited electrons won't be able to relax with the generation of secondary phonons – they will emit photons, and the emission will be at maximum.

Substituting the numerical values of the quantities ($v_{\rm L}^* \approx 10^5$ cm/s; FWHM ≈ 2.8 meV), we obtain an estimate of the chord length providing the maximum intensity of spontaneous emission of photons: $H < 1.2$ nm. Since $H \leq D$, the estimate for the diameter $D < 1.2$ nm would be a valid condition to yield yet an appreciable spontaneous emission of photons, in a situation when the vibration levels are separated (by ΔE_H, cf. Fig. 6) quite sparsely. With an increase in the diameter of a gold nanoparticle from 1.2 nm to 8 nm, the splitting between the levels will decrease and eventually cease at $D \approx 8$ nm. It is by the spontaneous emission of THz photons that we explain the nature of the catalytic activity observed in gold nanoparticles with a diameter less than 8 nm[22–24] (see Table 5); the idea is that the emission of THz photons promote the catalysis of chemical reactions on the surface of gold nanoparticles. The emission of photons will be accompanied by cooling of the nanoparticles insofar as they are not thermally insulated.

The cessation of photon emission at $D \approx 8$ nm can also be a manifestation of the energy dissipation of an excited electron due to its multiple scattering by other electrons, if the nanoparticle size becomes comparable to the average electron mean free path in the nanoparticle. Judging by the experimental data on the catalytic activity of gold nanoparticles depending on their diameter,[22–24] the average electron mean free path in gold nanoparticles is not less than 8 nm.

The higher the multiplicity of laying the energy step of the longitudinal phonons ΔE_D within the FWHM width, that is, the larger the FWHM/ΔE_D ratio, the higher the probability of superposition of the energy level expanded to δE on the level of the primary phonon, which will lead to electron relaxation with the generation of a secondary phonon (with energy of the primary phonon). And the lower the intensity of spontaneous emission of photons, the lower the catalytic activity of the nanoparticle and the lower the degree of its cooling.

REFERENCES

[1] Moldosanov, K. A., Lelevkin, V. M., Kozlov, P. V., and Kaveev, A. K., "Terahertz-to-infrared converter based on metal nanoparticles: potentialities of applications," *Journal of Nanophotonics* **6**, 061716 (2012).

[2] Kaveev, A. K., Moldosanov, K. A., Lelevkin, V. M., Kozlov, P. V., Kropotov, G. I., and Tsypishka, D. I., "Device for imaging terahertz radiation sources. Russian patent RU 2511070. Priority: 01.10.2012, date of publication: 10.04.2014 (Bull. 10)." https://patents.google.com/patent/RU2511070C1/en (2012). Accessed : 18 August 2021.

[3] Moldosanov, K. A., Lelevkin, V. M., Kairyev, N. Z., and Kaveev, A. K., "Terahertz-to-infrared converter. Patent of the Kyrgyz Republic No. 1684 dated 19 August 2013." Bulletin "Intellectualdyk Menchik – Intellectual Property" No. 10 (187), pp. 7-8, October 2014. Bishkek, 2014. (in Kyrgyz and Russian languages), http://test.patent.kg/doc/im/2014/10.pdf (2014). Accessed : August 18, 2021.

[4] Moldosanov, K. A., Postnikov, A. V., Lelevkin, V. M., and Kairyev, N. J., "Terahertz imaging technique for cancer diagnostics using frequency conversion by gold nano-objects," *Ferroelectrics* **509**(1), 158 (2017).

[5] Postnikov, A. V., Moldosanov, K. A., Kairyev, N. J., and Lelevkin, V. M., "Prospects for terahertz imaging the human skin cancer with the help of gold-nanoparticles-based terahertz-to-infrared converter," in [*Fundamental and Applied Nano-Electromagnetics II*], Maffucci, A. and Maksimenko, S. A., eds., *NATO Science for Peace and Security Series B: Physics and Biophysics*, 151, Springer, Dordrecht, The Netherlands (2019). Proceedings of the NATO Advanced Research Workshop on Fundamental and Applied NanoElectroMagnetics II: THz Circuits, Materials, Devices. Minsk, Belarus, 5-7 June, 2018.

[6] Moldosanov, K. A., Lelevkin, V. M., Kairyev, N. Z., and Postnikov, A. V., "Terahertz-infrared converter for visualiation of sources of terahertz radiation. Russian patent RU 2642119. Priority: 21.06.2016, date of publication: 24.01.2018 (Bull. 3)." http://www1.fips.ru/fips_servl/fips_servlet?DB=RUPAT&DocNumber=2642119&TypeFile=html (2016). Accessed : August 18, 2021.

[7] Postnikov, A. V., Moldosanov, K. A., Kairyev, N., and Lelevkin, V., "A device to inspect a skin cancer tumour in the terahertz range, transferring the image into the infrared," *EPJ Web Conf.* **195** (2018).

[8] Moldosanov, K. A., Postnikov, A. V., Lelevkin, V. M., and Kairyev, N. J., "Prospects of designing gold-nanoparticles-based soft terahertz radiation sources and terahertz-to-infrared converters for concealed object detection technology," in [*Millimetre Wave and Terahertz Sensors and Technology XII*], Salmon, N. A. and Gumbmann, F., eds., **11164**, 11640B, International Society for Optics and Photonics, SPIE (Oct 2019).

[9] "Infrared Cameras Inc., Mirage 640 P-series | fixed / process control calibrated thermal camera with temperature measurement." https://infraredcameras.com/thermal-infrared-products/mirage-640-p-series/. Accessed: August 6, 2018.

[10] Tanner, D. B., Sievers, A. J., and Buhrman, R. A., "Far-infrared absorption in small metallic particles," *Phys. Rev. B* **11**, 1330–1341 (Feb 1975).

[11] Granqvist, C. G., Buhrman, R. A., Wyns, J., and Sievers, A. J., "Far-infrared absorption in ultrafine Al particles," *Phys. Rev. Lett.* **37**, 625–629 (Sep 1976).

[12] Gor'kov, L. P. and Eliashberg, G. M., "Minute metallic particles in an electromagnetic field," *Sov.Phys. JETP* **21**, 940 (Nov 1965). J. Exptl. Theoret. Phys. (U.S.S.R.) 48, 1407–1418 (May 1965).

[13] Glick, A. J. and Yorke, E. D., "Theory of far-infrared absorption by small metallic particles," *Phys. Rev. B* **18**, 2490–2493 (Sep 1978).

[14] Gilat, G. and Nicklow, R. M., "Normal vibrations in aluminum and derived thermodynamic properties," *Phys. Rev.* **143**, 487–494 (Mar 1966).

[15] Granqvist, C. G., "Far infrared absorption in ultrafine metallic particles: Calculations based on classical and quantum mechanical theories," *Z. Phys. B* **30**, 29–46 (Mar 1978).

[16] Postnikov, A. and Moldosanov, K., "Phonon-assisted radiofrequency absorption by gold nanoparticles resulting in hyperthermia," in [*Fundamental and Applied Nano-Electromagnetics*], Maffucci, A. and Maksimenko, S. A., eds., *The NATO Science for Peace and Security Programme, Series B: Physics and Biophysics*, 171 – 201, Springer, Dordrecht, The Netherlands (2016). Proceedings of the NATO Advanced Research Workshop on Fundamental and Applied Electromagnetics, Minsk, Belarus, 25-27 May, 2015.

[17] Moldosanov, K. and Postnikov, A., "On the plausible nature of the size effect in heterogeneous catalysis on gold nanoparticles." https://arxiv.org/abs/1808.10607 (2018).

[18] Dal Corso, A., "Ab initio phonon dispersions of transition and noble metals: effects of the exchange and correlation functional," *J. Phys. Condens. Matter* **25**, 145401 (Apr 2013).

[19] Kargin, V. A. (Chief editor) et al., [*Encyclopedia of Polymers. Volume 1 (in Russian)*], p. 443, "Soviet Encyclopedia" Publishers, Moscow (1972).
[20] Wallace, V. P., Fitzgerald, A. J., Pickwell, E., Pye, R. J., Taday, P. F., Flanagan, N., and Ha, T., "Terahertz pulsed spectroscopy of human basal cell carcinoma," *Applied Spectroscopy* **60**, 1127 (Oct 2006). PMID: 17059664.
[21] Pickwell, E. and Wallace, V. P., "Biomedical applications of terahertz technology," *Journal of Physics D: Applied Physics* **39**, R301 (Sep 2006).
[22] Hutchings, G. J. and Haruta, M., "A golden age of catalysis: A perspective," *Applied Catalysis A: General* **291**(1), 2 (2005). Catalysis by Gold.
[23] Haruta, M., "When gold is not noble: Catalysis by nanoparticles," *The Chemical Record* **3**, 75 (Apr 2003).
[24] Haruta, M., "Size- and support-dependency in the catalysis of gold," *Catalysis Today* **36**, 153 (Apr 1997).